Stellarator Flexibility Options with Variable Modular Coil Currents

D. A. Spong, D.J. Strickler, S.P. Hirshman, J.F. Lyon, L.A. Berry, D. Mikkelsen[1],

D. Monticello[1], A. S. Ware[2]

Oak Ridge National Laboratory, P.O. Box 2009, Oak Ridge, TN 37831-8073
[1]Princeton Plasma Physics Laboratory, P.O. Box 451, Princeton, NJ 08502
[2]Department of Physics and Astronomy, University of Montana, Missoula, MT, 59812

Recently developed stellarator optimization tools[1] have successfully merged the external coil-plasma boundary optimization with the internal plasma boundary physics optimization steps. Besides allowing better control over the engineering features and complexity of the magnet coils (and thus lower cost) in an ongoing design, this procedure also allows one to more methodically explore the physics flexibility options in a completed design where the coil geometry has become fixed, but the coil currents can still be varied over some specified range. This type of flexibility is one of the significant advantages that stellarators can offer over tokamaks. Developing better tools for exploring the available parameter space can enhance the scientific value of a stellarator experiment.

As an example of such flexibility studies, we analyze the QPS (quasi-poloidal stellarator) device[2], which has been designed with independent power supplies for controlling the five unique modular coil groups; the three vertical field coil pairs; and the toroidal field coils. In addition, the plasma current can be considered as an independent variable, since an Ohmic transformer is available to drive plasma current. After using one of the modular coil currents as a normalizing parameter, there are still nine independent parameters. Since searches of even a nine-dimensional parameter space, based on intuition or trial and error, are likely to miss interesting combinations, we have used the merged coil–plasma optimizer code to automate this search process. In the following, we focus on transport improvement and island avoidance at low β, but such techniques can also be applied to stability optimization targets at finite β.

Coil configuration

QPS is a compact ($R_0/\langle a \rangle = 2.7$) two-field period stellarator that maintains a dominant poloidal symmetry in its magnetic field strength variation. The current reference design for QPS is based on a set of 20 modular field coils (with 5 unique coil shapes), six vertical field coils, and 12 toroidal field coils. In Figure 1 the full set of coils are shown along with the plasma outer flux surface. In Figure 2 shows only the plasma outer flux surface for the reference configuration and the modular coils.
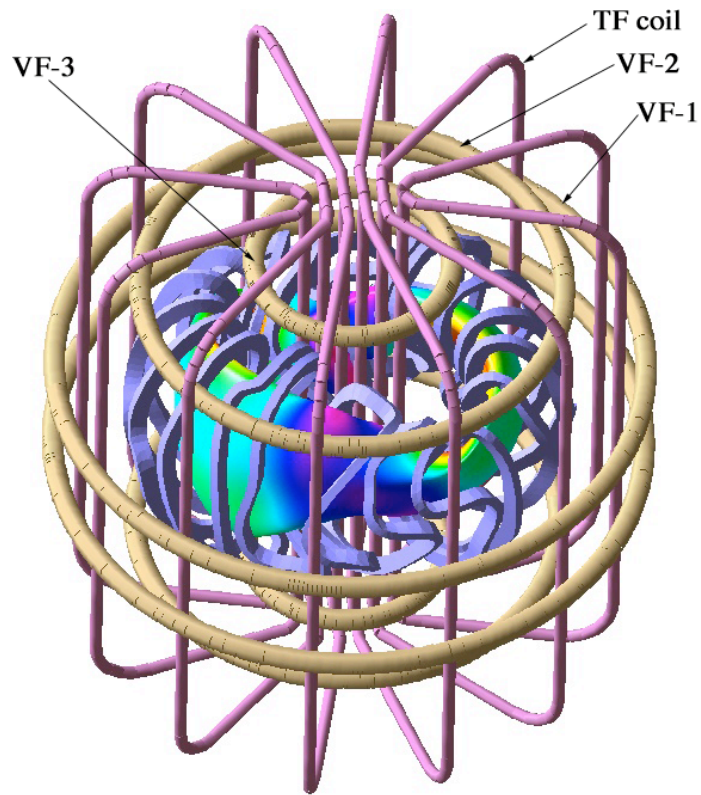
Figure 1 – QPS Coil-sets and plasma. Modular coils are shown in light blue, toroidal field coils are pink, vertical field coils are in tan. Color contours (blue!=!low field, red = high field) show the magnetic field strength on the outer plasma magnetic flux surface.
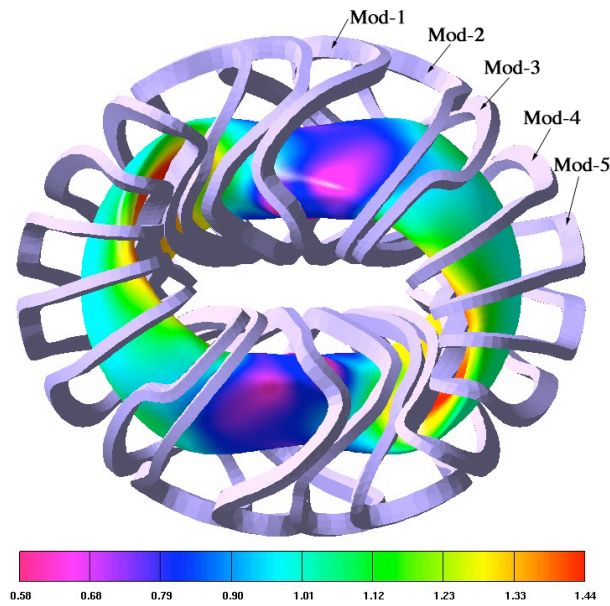

Figure 2 - QPS outer plasma surface and modular magnetic field coils.

The coil current optimization will vary the currents in modular coils, vertical field coils and the toroidal field coils. Stellarator symmetry is maintained by keeping the currents in each unique modular coil group equal. Engineering constraints will limit the range over which these currents can be varied; the current constraints that we assume are listed in table 1. The current values given for the toroidal field coil (TF) are for the total current flowing through the 12 TF coils; the other currents apply to individual coils. It should also be noted that in an experimental device some component of the vertical field coil currents are required for plasma positioning and compensation of stray fields from the Ohmic transformer. We will not directly assess the latter current requirements in this study, but will check that the plasma-coil separation does not become too small.

Table 1 - Minimum, maximum and reference current levels for our flexibility study.

Coil	Mod 2	Mod 3	Mod 4	Mod 5	VF 1	VF 2	VF 3	TF
Minimum current (kAmps)	0	0	0	0	-60	-180	-130	-75
Maximum current (kAmps)	380	380	380	380	+60	+180	+130	+75
Reference design current (kAmps)	300	300	300	300	0	-75.5	-129	-24.9

Transport Optimization

As a first example of coil current optimization, we will find current distributions that can either improve or degrade the neoclassical transport properties of QPS. A number of transport measures are available for this purpose, including: the effective ripple from the NEO[3] code; collisional transport coefficients from the DKES[4] code; quasi-poloidal symmetry; and centering of J* (longitudinal adiabatic invariant), B_{min}, and B_{max} contours[5]. The primary target we will focus on in this article is the effective ripple provided by the NEO[3] code. Work is underway on some of the other targets, but this is not yet complete. Control over the effective ripple has so far had the most direct correlation with other measures of transport such as DKES and global Monte Carlo lifetime estimates. We have also been able to improve quasi-poloidal symmetry by a factor of 4–5 over the reference design, but this has proven to be anti-correlated with other transport measures. This characteristic is possibly related to the path that the optimizer chooses for QP-symmetry improvement which is to increase currents in the corner section modular coils (Mod-4,5) and weaken currents in the side modular coils (Mod-2,3). This increases the ripple level and the fraction of trapped particles; over this range of parameters these effects seem to have a more negative impact than the positive effect from the symmetry improvement.

In Figure 3 the range of effective ripple coefficients that has been obtained by targeting either improved or degraded transport is plotted as a function of flux surface.
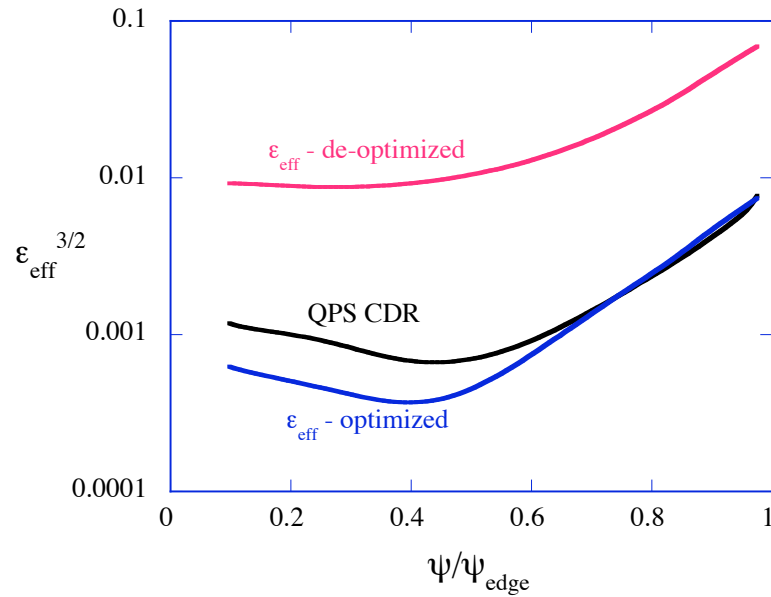

Figure 3 – Effective ripple coefficient as a function of normalized toroidal flux for the reference configuration (QPS CDR) and for improved (red) and degraded (blue) configurations.
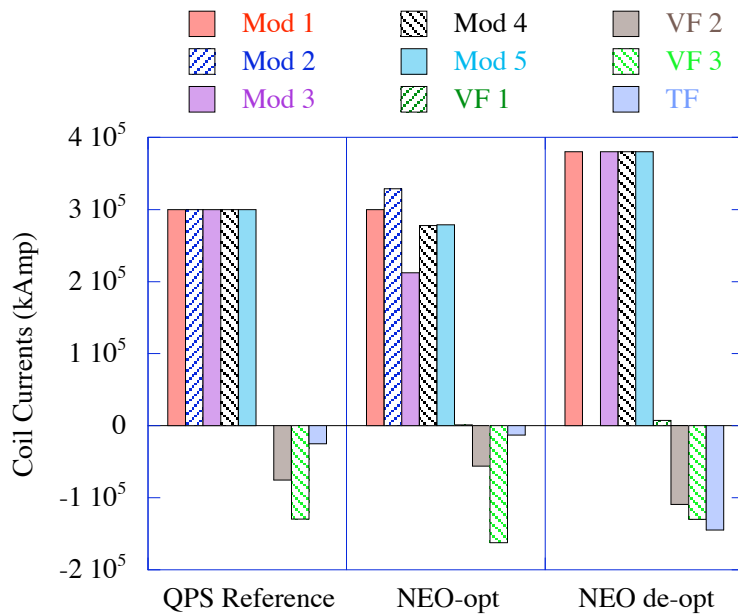

Figure 4 - Coil current distributions for transport optimized and de-optimized cases.

Figure 4 shows a histogram of the coil current distributions that produce the configurations used in Figure 3. As can be seen, decreases in effective ripple are obtained by raising the current in the middle Mod-2 coil, and lowering it in the Mod-3, -4, -5 coils going into the corner section. In order to increase the effective ripple, the optimizer chooses to zero out the current in the Mod-2 coil and run currents in the Mod-1, 3, 4, and 5 coils up to their limits (in this case, we allowed currents in all of the modular coils to be varied). Coil-plasma separations have not been changed too significantly by these optimizations; for the reference configuration, the minimum coil-plasma separation is 13.2 cm - it becomes 11.9 cm for the NEO optimized case and 13.9 cm for the NEO de–optimized case. These optimizations have been carried out using the Levenberg-Marquardt (LM) option of the STELLOPT optimizer. Coil current optimization attempts have also been made using differential evolution (DE) and genetic algorithm (GA) options. The DE and GA approaches allow the coil current limits to be naturally incorporated into the calculation as bounds upon the search process, but to date have not resulted in configurations with good flux surfaces. The LM algorithm does not provide any direct way to constrain the values accessed by coil currents and, at this time, requires user intervention or constraint-related targets to accomplish this. Typically one runs the LM method for a certain number of iterations, finds that one or more of the coil currents has gone outside of its acceptable range, fixes these coil currents at whichever bound is closest (i.e., maximum/minimum value), restarts the LM algorithm using the reduced number of coils, checks again, etc.

The effectiveness of the above optimization/de-optimization of transport has been further checked by using other measures of transport. We have run the DKES[4] code, which calculates collisional transport coefficients, and the DELTA5D[6] Monte Carlo code, which calculates global energy lifetimes.
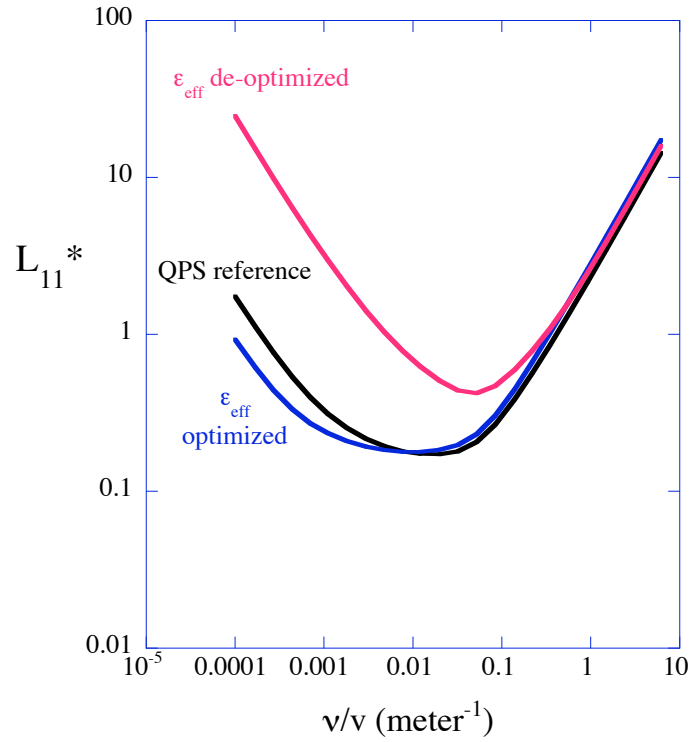
Figure 5 - DKES mono-energetic transport coefficient vs. collisionality for the reference, effective ripple optimized and de-optimized cases (for $E_r = 0$).

In Figure 5 DKES transport coefficients are plotted for a half radius flux surface and with $E_r = 0$ (in order to better show configurational differences). At low collisionalities (below plateau, $\nu/v < 0.02$) these show similar variations with optimization as the effective ripple coefficient shown in Figure 3. In the higher collisionality regime, there is not as much sensitivity to the configuration.
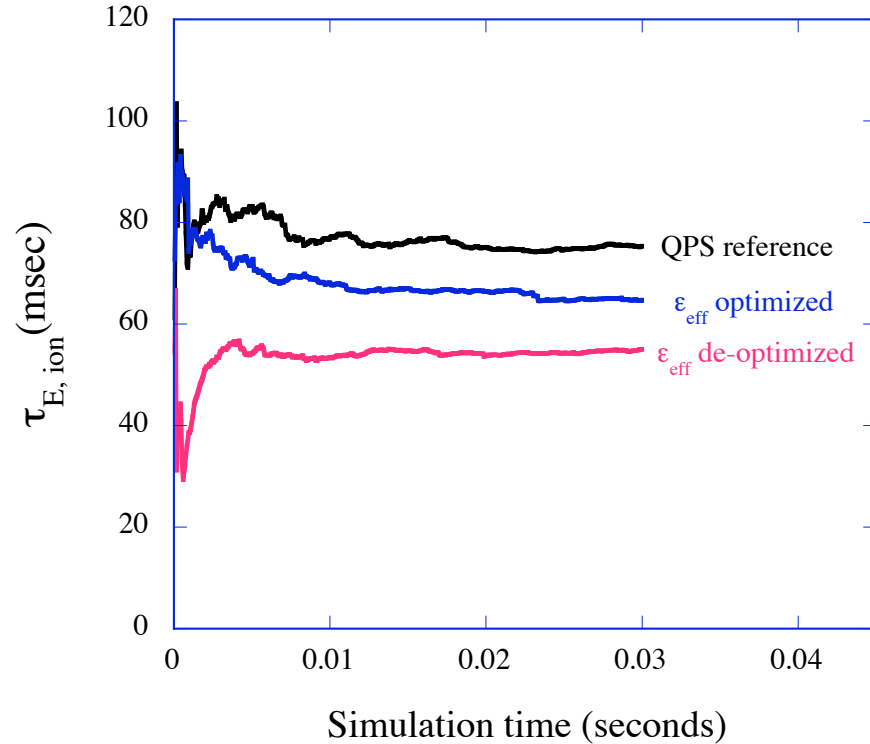
Figure 6 - Monte Carlo global energy lifetimes for reference, transport de-optimized, and optimized configurations.

Figure 6 shows the Monte Carlo ion energy lifetimes for the reference, de-optimized and optimized configurations for the plasma parameters: $T_{electron}(0) = 0.5$ keV, $T_{ion}(0) = 0.5$ keV, and $n(0) = 8.3 \times 10^{19}$ m^{-3}. These parameters are expected to be typical of the QPS ICRH-heated regime. This figure indicates that the optimized configuration has lifetimes in between the reference and de-optimized configurations. There is also some tendency towards this behavior in the plateau and higher collisionalities of Figure 5, but this differs from the low collisionality behavior. The Monte Carlo lifetimes do not assume diffusive transport and take into account transport properties over the entire volume and for a Maxwellian distribution while the DKES results of Figure 5 are monoenergetic and evaluated at a fixed flux surface. Nevertheless, both results show that a significant variation in confinement can be accessed by coil current optimization.

Island Avoidance

In addition to variations in the coil currents for confinement optimization, we have also carried out similar optimizations in order to control the shape of the rotational transform profile. The goal here has been to use combinations of Ohmically driven plasma current and modifications in the coil current distributions in order to keep the iota profile bounded in between windows determined by the adjacent rational surfaces (which occur for QPS at iota = 2/8, 2/7, 2/6, 2/5, etc.). Once such configurations are found, they are checked by use of the PIES code[7]. If good surfaces are found then the search ends; if large islands are present, further optimizations are performed to avoid whatever resonance has entered into the plasma. As there is generally some deviation between the rotational transform predicted by VMEC and that given by PIES, several iterations of this process may be required to find a satisfactory configuration. In the operation of low aspect ratio stellarator devices, this type of search for optimum plasma and coil current distributions for island avoidance is expected to be of importance in finding attractive regimes of operation. It may also be possible to more directly target island formation through targeting measures such as radial magnetic field components, parallel currents, etc. at the island locations.

We have optimized vacuum configurations with most of the weight placed on the target of attaining a specific rotational transform profile. For the results presented here, the transport properties have then been checked a posteriori, indicating that, in addition to decreased island sizes, the new configurations generally lead to improved confinement. The coil current optimizations have been carried out with varying levels of Ohmic current present; the Ohmic current profile has been modeled as centrally peaked. By combining the coil current optimization with finite plasma current levels, we have been able to both raise the rotational transform profile and flatten it at the same time.
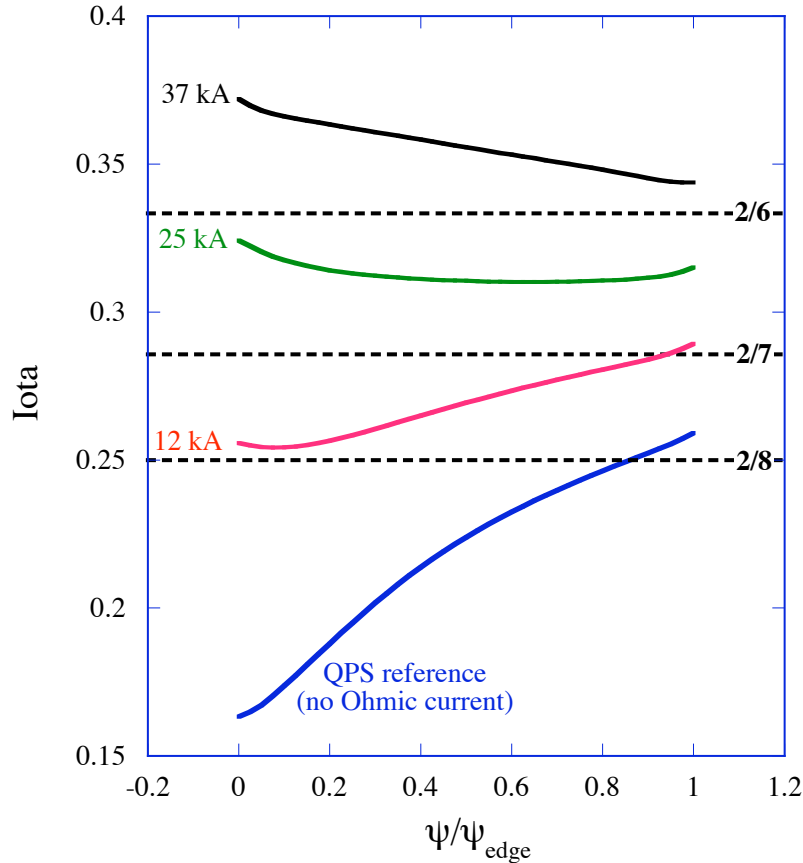
Figure 7 – QPS rotational transform profiles that have been attained through combinations of Ohmic plasma current and coil current optimization.

Figure 7 shows some of the VMEC rotational transform profiles that we have obtained by this procedure. Of these profiles, only the 25 kA has resulted in good surfaces so far. The 37 kA profile generated 4/11 islands that destroyed the outer part of the plasma while the 12 kA case generated 2/7 islands. With further iterations between the optimizer and PIES, it should be possible to also avoid major islands in the 12 and 37 kA cases. Figure!8 shows the coil current distributions that were used to produce the above cases; note that the 12 kA and 25 kA cases use the same coil currents—only the plasma current has been changed. In Figure 9, the surfaces obtained from the PIES code are shown for the 25 kA case, indicating that islands have been effectively minimized by this procedure. The 25!kA optimized case had a minimum coil-plasma separation of 14.6 cm as compared to 13.2 cm in the reference case.
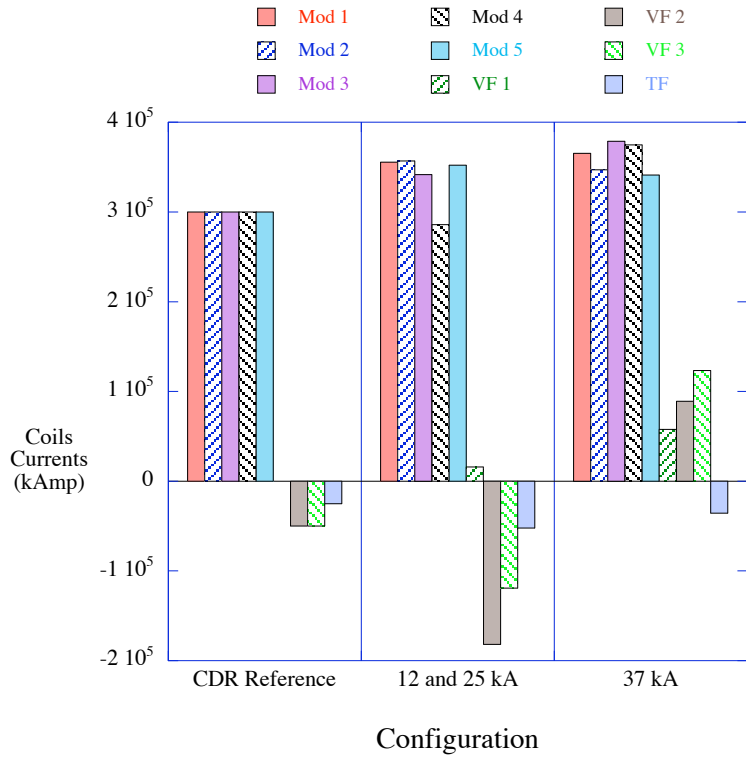
Figure 8 - Coil current distributions for the rotational transform profiles shown in Figure 7.
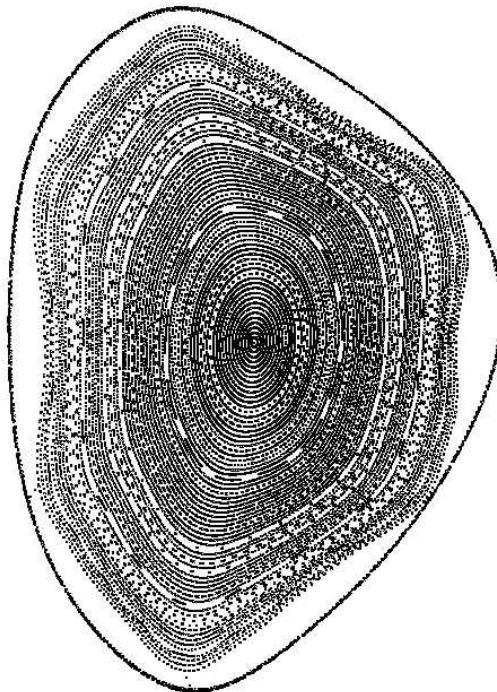

Figure 9 - PIES magnetic surfaces for the coil current optimized case with 25 kA. The transform profile is constrained to remain between the 2/6 and 2/7 resonances.

Conclusions

Physics flexibility is an important aspect of stellarator experiments. We have demonstrated a new way to methodically search for configurations that sample extremes of transport and that minimize low β islands using the STELLOPT optimizer. This approach is especially useful when individual modular coil group currents can be varied as well as vertical and toroidal field coil currents. In the case of the QPS device, coil current distributions have been found that result in up to a factor of ~30 variation in low collisionality transport. Also, the transform profile can be regulated to remain between adjacent rationals, resulting only in island chains of very limited width. Similar techniques should be applicable to other optimization targets, such as stability.

[1] D. J. Strickler, et al., to be published in Fusion Science and Technology, 2003.

[2] J. F. Lyon, et al., "Overview of the QPS Project," and D. A. Spong, et al., "Confinement Physics of Quasi-Poloidal Stellarators," 30th European Physical Society Conf. On Controlled Fusion and Plamsa Physics, St. Petersburg, Russia, July 7-11, 2003.

[3] V. V. Nemov, S. V. Kasilov, W. Kernbichler, M. F. Heyn, Phys. Plasmas **6**, 4622 (1999).

[4] W. I. van Rij, S. P. Hirshman, Phys. Fluids B, **1** (March, 1989).

[5] Rome, NF

[6] D, A. Spong, S. P. Hirshman, L. A. Berry, J. F. Lyon, et al., Nuclear Fusion **41**, 711 (2001).

[7] A. Reiman and H. S. Greenside, *J. Comput. Phys.* **75** (1988) 423.